

Multiple carriers of Q noble gases in primitive meteorites

Yves Marrocchi^{1,2,*}, Guillaume Avice^{1,2} & Nicolas Estrade^{1,2,3}

Submitted on 31 Jan. 2015, Accepted for publication on 05 March 2015

¹ Université de Lorraine, Vandoeuvre-lès-Nancy, F-54501, France

² CNRS, CRPG, UMR 7358, Vandoeuvre-lès-Nancy, F-54501, France

³ PCIGR, EOS, University of British Columbia, Vancouver, BC, Canada

* Corresponding author's email: yvesm@crpg.cnrs-nancy.fr

Key points

- Noble gas isotopic fractionation
- Origin of meteoritic noble gases
- Evolution of the accretion disk

Abstract

The main carrier of primordial heavy noble gases in chondrites is thought to be an organic phase, known as phase Q, whose precise characterization has resisted decades of investigation. Indirect techniques have revealed that phase Q might be composed of two subphases, one of them associated with sulfide. Here we provide experimental evidence that noble gases trapped within meteoritic sulfides present chemically- and thermally-driven behavior patterns that are similar to Q-gases. We therefore suggest that phase Q is likely composed of two subcomponents: carbonaceous phases and sulfides. *In situ* decay of iodine at concentrations levels consistent with those reported for meteoritic sulfides can reproduce the ^{129}Xe excess observed for Q-gases relative to fractionated Solar Wind. We suggest that the Q-bearing sulfides formed at high temperature and could have recorded the conditions that prevailed in the chondrule-forming region(s).

Index terms: 0343, 1027, 1028, 1029.

Keywords: noble gases, meteorites, phase Q, isotopic fractionation, chondrules, accretion disk.

1. Introduction

Primordial noble gases trapped in chondrites are concentrated in residues obtained after demineralization by HF/HCl of the respective bulk meteorites [Lewis *et al.*, 1975]. Most of the heavy noble gases (Ar, Kr & Xe) and a small amount of He and Ne are readily released from the original HF/HCl residues by HNO₃ oxidation. This discovery led to the operational definition of phase Q, the oxidisable carrier of primordial noble gases (hereafter Q-gases), which has been found to be ubiquitous in different classes of chondrites [Busemann *et al.*, 2000; Huss *et al.*, 1996]. The nature of phase Q is still under debate but it likely corresponds to carbonaceous structures as noble gas abundances released from acid residues by stepped combustion correlate with those of carbon [Ott *et al.*, 1981]. However, despite the consensus on the carbonaceous nature of phase Q the phase has not yet been isolated from acid residues [Amari *et al.*, 2013]. Nevertheless, indirect techniques have enabled characterization of Q-gases and have revealed: (i) a high noble gas concentration [Huss *et al.*, 1996], (ii) a significant fractionation relative to the solar composition in favor of heavy elements and isotopes [Busemann *et al.*, 2000] and (iii) a common high gas-release temperature for all noble gases in the range 1000-1200°C for unaltered chondrites [Huss *et al.*, 1996]. In addition, several studies indicated that phase Q may consist of two subcomponents: Q₁ which is readily soluble in HNO₃ and contains most of the heavy noble gases; and Q₂ which dissolves slowly in hot concentrated HNO₃ [Busemann *et al.*, 2000; Gros and Anders, 1977; Marrocchi *et al.*, 2005a]. It has been proposed that at least one of these subcomponents might be related to sulfides [Gros and Anders, 1977] but no study has specifically investigated this possibility. However, recent studies report striking results that also suggest that sulfides may have been underestimated as a potential subcarrier of Q-gases. Troilite (FeS) from iron meteorites reproduces the thermal behavior of phase Q well, with a common release temperature of 1000-1200°C for all noble gases [Nishimura *et al.*, 2008]. In addition, stepped

combustion measurements on CR chondrites have revealed that very little carbon is associated with Q-gases, suggesting that phase Q might not be solely carbonaceous [Verchovsky *et al.*, 2012]. Furthermore, study of the microdistribution of noble gases within ordinary chondrites has revealed that the sulfide coatings surrounding chondrules exhibit Ne and Ar concentrations at the Q-level as well as Q-like elemental ($^{36}\text{Ar}/^{20}\text{Ne}$) and isotopic ($^{38}\text{Ar}/^{36}\text{Ar}$) ratios [Vogel *et al.*, 2004]. Here we report results from an experimental study in which the same chemical treatments as those used for the isolation of phase Q (HF/HCl treatment) and the release of Q-gases (HNO_3 oxidation) were applied to iron sulfides separated from the Mundrabilla iron meteorite (IAB). We also test the possibility that sulfides could contribute significantly to the ^{129}Xe and $^{131,132,134,136}\text{Xe}$ excesses observed for Xe-Q relative to fractionated solar wind.

2. EXPERIMENTAL DETAILS

2.6 g of pyrrhotite ($\text{Fe}_{0.98}\text{S}$) extracted from a fragment of the Mundrabilla iron meteorite (Naturmuseum Senckenberg - Frankfurt - Germany) was ground and separated into two fractions. The first fraction (FeS) was set aside (without undergoing chemical treatment) in order to determine the noble gas content of the Mundrabilla's pyrrhotites. The second fraction was immersed for 24 hours in a HF/HCl, 0.1/1, v/v mixture at 70°C and under nitrogen flow [Piani *et al.*, 2012]. After HF/HCl treatment, the sample was washed with water, thoroughly dried at 50°C and then separated into two equal aliquots. One aliquot was retained for noble gas analysis (hereafter FeS-HCl) while the other was etched with 14 M HNO_3 for 24 hours at 70°C and under nitrogen flow [Lewis *et al.*, 1975]. The resulting etched residue (FeS- HNO_3) was washed with water and dried at 50°C before analysis. The FeS- HNO_3 fraction exhibits a reddish color that is distinct from the gray color of both the starting material and the HF/HCl residue.

Ar, Kr and Xe were measured in the raw sample, HF/HCl residue, and nitric-etched residue. Samples were weighed, wrapped in platinum foil and then loaded into a glass sample-tree. The samples were gently baked at 150°C for three days in order to remove adsorbed atmospheric gases. Noble gases were extracted by stepped pyrolysis in the temperature range 300-1768°C using a tungsten coil. The linear current-temperature calibration curve for the coil was obtained using an optical pyrometer with a precision of $\pm 25^\circ\text{C}$ for temperatures above 800°C. The calibration curve was extrapolated to temperatures lower than 800°C. Extraction times were adjusted as function of temperature: (i) 15 min for the four low-temperature steps (i.e., 300-1300°C), (ii) 12 min for the 1500°C step and (iii) 5 min for the final step (at the platinum melting-point: 1768°C). The released gases were exposed to three consecutive pellet getters containing SAES St172 getter alloy in order to remove active gases (10 min at 450°C, 10 min at room temperature). Ar, Kr and Xe were held on a charcoal finger at liquid nitrogen temperature for 45 minutes, then the residual light noble gases were pumped out over 5 min. Active charcoal immersed in liquid nitrogen was then heated to -105°C using an electric wire that surrounds the charcoal. Calibration curves determined from air standards showed that Kr and Xe are not affected at this temperature while 70 % of the Ar is released. This procedure reduces the amount of Ar in the mass spectrometer, which has a considerable effect on the mass discrimination of krypton and xenon. Argon released from the charcoal finger was then pumped out for 5 min. The liquid nitrogen was then removed and the charcoal finger was heated to 250°C for 25 min to release Xe, Kr and the residual fraction of Ar. Heavy noble gases were then introduced into high sensitivity pulse-counting static mass spectrometer (Washington University, Saint Louis, USA, [Mabry *et al.*, 2007; Meshik *et al.*, 2007]) for determination of Ar, Kr, and Xe abundances and $^{38}\text{Ar}/^{36}\text{Ar}$, $^{86}\text{Kr}/^{84}\text{Kr}$, and $^{129}\text{Xe}/^{132}\text{Xe}$ isotopic ratios.

Hot blanks (1200°C) were performed several times during each analytical session. The Kr and Xe concentrations within Pt foils were also measured and appeared to be negligible. The measured Kr and Xe abundances are typically accurate to better than 5% whereas the Ar concentrations present a lower precision of $\approx 25\%$ and are not presented here. The uncertainties in the $^{86}\text{Kr}/^{84}\text{Kr}$ and $^{129}\text{Xe}/^{132}\text{Xe}$ isotopic ratios (1σ) include hot blank, standard and sample uncertainties (Table 1).

3. RESULTS

The stepwise-heating analysis show that pyrrhotite releases Kr and Xe at temperatures between 900 and 1768°C, with a maximum release occurring in the range 900-1175°C (Fig 1; Table 1). The total concentration of ^{132}Xe measured in the Mundrabilla's pyrrhotite was $3.27 \cdot 10^{-10} \text{ cm}^3 \text{ STP.g}^{-1}$, while the ^{84}Kr concentration was slightly higher ($9.21 \cdot 10^{-10} \text{ cm}^3 \text{ STP.g}^{-1}$). $^{86}\text{Kr}/^{84}\text{Kr}$ ratios measured for each temperature step present homogenous values close to the atmospheric composition (Table 1). $^{129}\text{Xe}/^{132}\text{Xe}$ ratios show more important variations with a clear excess of radiogenic ^{129}Xe in all except the final extraction steps that lies close to the atmospheric composition (Table 1). These results are consistent with previous reports of Kr and Xe concentrations within troilites from iron meteorites [*Mathew and Marti, 2009; Nishimura et al., 2008*]. No significant mass variation was observed following the HF/HCl treatment but the FeS-HCl residues displayed a significant gas loss compared to the initial material, both for Kr ($\approx 53\%$) and Xe ($\approx 38\%$; Fig 1; Table 1). However, Kr and Xe did present the same thermal release patterns as the original sample, with the maximum noble gas release occurring in the range 1000-1200°C (Fig. 1). $^{86}\text{Kr}/^{84}\text{Kr}$ and $^{129}\text{Xe}/^{132}\text{Xe}$ ratios are similar to the original sample (Table 1). The FeS-HNO₃ residue displayed a reddish color that was distinct from the gray color of the starting material and the HF/HCl residue, but no mass variation was observed compared to the initial material. The amounts of Kr and Xe released

from the FeS-HNO₃ residue are much lower than those from the FeS-HCl fraction, with gas losses of 65% and 69% recorded for Kr and Xe, respectively (Fig 1; Table 1). Stepwise-heating analyses revealed that all of the temperature steps were affected by the degassing of Kr and Xe (Fig. 1). ¹²⁹Xe/¹³²Xe ratios show resolvable but lower excess of radiogenic ¹²⁹Xe comparing to the other residues (Table 1).

4. DISCUSSION

Significant degassing was observed upon HF/HCl treatment, suggesting that sulfides are sensitive to chemical digestion (Fig. 1). However, HF/HCl-treated pyrrhotite still contains a significant amount of Kr and Xe and could thus be considered as an acid-resistant mineral. This is confirmed by TEM observations of meteoritic acid residues that contain an important amount of inorganic material such as sulfides and oxides [Derenne and Robert, 2010]. In addition, our results indicate that pyrrhotite has a strong susceptibility to HNO₃ oxidation (Table 1). This feature has also been reported for pentlandite (i.e., (Fe,Ni)₉S₈) but pentlandite differs from phase Q in its thermal stability with decomposition starting at 610°C [Kerridge *et al.*, 1979]. In contrast, the release pattern of noble gases trapped within pyrrhotite closely resembles that of the Q-gases, with a major release of Kr and Xe occurring between 900 and 1200°C (Fig 1). Similar results were obtained for each of the five noble gases released from troilite from the Saint Aubin iron meteorite (UNGR) [Nishimura *et al.*, 2008], demonstrating that nickel-poor iron sulfides match the thermal characteristics of phase Q. The high temperature release is directly linked to the incongruent dissociation of pyrrhotite, which occurs in the range 1000-1200°C, depending on the stoichiometry [Kellerud, 1963]. Hence, our results suggest that chondritic sulfides could (i) represent a plausible subcarrier of Q-gases and could (ii) contribute to the Q-gas budget at the maximum-release temperature of Q-gases (i.e., 1000-1200°C) [Huss *et al.*, 1996]. This is in good agreement with sulfides

separated from Allende (CV3) that show typical Xe-Q isotopic compositions at high temperature (i.e., > 900°C), representing few percent of the total Xe-Q reported for this chondrite [Busemann *et al.*, 2000; Lewis *et al.*, 1977]. It might be argued that the amounts of Kr and Xe measured in iron sulfides from the Mundrabilla iron meteorite are three orders of magnitude lower than those reported in phase Q [Busemann *et al.*, 2000; Huss *et al.*, 1996]. However, the goal of this study was not to isolate phase Q as iron meteorites do not show this noble gas component (except in rare graphite nodules, [Matsuda *et al.*, 2005]) but rather to test the chemical sensitivity and the thermal behavior of noble gas-bearing sulfides. Consequently, we suggest that phase Q likely corresponds to complex Q-gas subcarriers of different natures: carbonaceous phases and iron sulfides.

Among the meteoritic noble gases, Xe-Q in different classes of chondrite is characterized by mass-dependent fractionation relative to solar wind (SW), favoring the heavy isotopes [Marrocchi and Marty, 2013; Meshik *et al.*, 2014]. However, clear excesses of ^{129}Xe and $^{131,132,134,136}\text{Xe}$ are also observed together with the mass-fractionated SW (Fig. 2a). These features are generally explained by a mixing model in which 98.4% of $\approx 8 \text{‰.amu}^{-1}$ mass-fractionated SW-Xe is mixed with 1.6% Xe-HL from nanodiamonds and monoisotopic ^{129}Xe from ^{129}I decay [Gilmour, 2010]. However, Xe-HL cannot contribute to Xe-Q release generated by on-line nitric oxidation of acid residues [Busemann *et al.*, 2000] because nanodiamonds are unaffected by etching [Crowther and Gilmour, 2013]. Hence, the $^{131,132,34,136}\text{Xe}$ excesses have been attributed to a gas carrier that presents the same enrichment in the light and heavy xenon isotopes as nanodiamonds but which has not yet been isolated [Gilmour, 2010]. Given our results, we can test an alternative explanation based on *in situ* fission and decay of $^{238}\text{U}+^{244}\text{Pu}$ and ^{129}I within sulfides. The mass fractionation of Xe-Q relative to SW-Xe and its associated uncertainty were determined for eight chondrites and for the average Q composition [Busemann *et al.*, 2000] using only the non-radiogenic/fissiogenic

Xe-Q isotopic ratios (i.e., $^{124,126,128}\text{Xe}/^{130}\text{Xe}$). According to the abundance of ^{129}Xe in phase Q [Busemann *et al.*, 2000], and assuming an initial solar system ratio of $1.1 \cdot 10^{-4}$ for $^{129}\text{I}/^{127}\text{I}$ [Gilmour *et al.*, 2006], we thus determined the iodine content required to correct the ^{129}Xe excess relative to the fractionated SW (Table 2). Then, on the basis of the abundances of $^{131,132,134,136}\text{Xe}$ in phase Q [Busemann *et al.*, 2000], we calculated the ^{238}U concentrations required to correct the excesses of $^{131,132,134,136}\text{Xe}$ relative to fractionated SW using the fission yields reported for ^{238}U and ^{244}Pu [Ragettli *et al.*, 1994], the branching ratio for ^{238}U and ^{244}Pu [Ozima and Podosek, 2002], the initial solar system ratios of $(^{244}\text{Pu}/^{238}\text{U})_0 = 6.8 \cdot 10^{-3}$ and $(^{238}\text{U}/^{235}\text{U})_0 = 137.88$ [Ozima and Podosek, 2002] and a start of radioactive decay 4.57 Gyr ago. Our results show that the respective ^{129}I and ^{238}U initial concentrations required to correct the ^{129}Xe and $^{131,132,134,136}\text{Xe}$ excesses relative to fractionated SW observed for Xe-Q across different chondrites [Busemann *et al.*, 2000] fall in the range of 0.03-0.45 ppm ^{129}I and 0-50 ppm ^{238}U (Table 2). The resulting iodine contents are in good agreement with the concentrations of 0.1-3.5 ppm reported for sulfides from different types of meteorites [Clark *et al.*, 1967; Goles and Anders, 1962]. Consequently, we propose that Q-gases trapped within sulfides could be responsible for the ^{129}Xe excess observed during the release of Q-gases. In contrast, the uranium contents required within sulfides to explain the $^{131,132,134,136}\text{Xe}$ excess relative to fractionated SW are generally too high compared to the sub-ppm concentrations reported for meteoritic sulfides [Croaz, 1979]. Moreover, the Xe-Q corrected for $^{238}\text{U}+^{244}\text{Pu}$ contributions does not produce a better fit for heavy xenon isotopes than the canonical model involving mixing of different Xe reservoirs [Meshik *et al.*, 2014] (Fig. 2b). Consequently, the excesses of ^{129}Xe could be attributed to the *in-situ* decay of ^{129}I within sulfides, while fission of $^{238}\text{U}+^{244}\text{Pu}$ would play a negligible role in generating the excess of $^{131,132,134,136}\text{Xe}$ relative to fractionated SW observed for Q-gases (Fig. 2a).

Q-gases are ubiquitous among the different types of chondrites, despite the fact that they experienced diverse secondary alteration processes such as fluid percolation and/or metamorphism [Bourot-Denise *et al.*, 2010; Brearley, 2006; Hewins *et al.*, 2014; Huss *et al.*, 2006; Marrocchi *et al.*, 2014]. This suggests that the formation of the S-rich subcarrier of Q-gases is linked to primary high-temperature processes rather than to parent body alteration. Recent reports have revealed that chondrule formation took place under high partial pressure of sulfur, leading to the formation of iron sulfide from the chondrule melts by solubility/saturation processes [Marrocchi and Libourel, 2013] and/or condensation at the surface of chondrules [Tachibana and Huss, 2005]. The formation of Q-bearing sulfides would be directly related to the chondrule-forming event. Such a view supports models which postulate that the formation of chondrules took place in an environment characterized by volatile-enriched gas that interacts at high temperature with chondrule precursor [Marrocchi and Libourel, 2013]. Thus, formation of Q-bearing sulfides can be achieved in regions characterized by enhancement of the respective noble gas partial pressures and under ionizing conditions that allow the isotopic fractionation observed for Q-gases relative to SW to be reproduced [Hohenberg *et al.*, 2002; Marrocchi *et al.*, 2005b; Marrocchi *et al.*, 2011].

5- Concluding remarks

We have performed an experiment to test whether iron sulfides might represent a plausible subcomponent of the main noble gas carriers in primitive meteorites - phase Q. Although significant noble gas degassing was observed upon HF-HCL treatment, our results show that noble gases trapped within sulfides present similar chemical susceptibility and thermal behavior than Q-gases. Hence, we propose that sulfides likely represent a plausible subcomponent of phase Q. Under this hypothesis, phase Q represents a mix of multiple

primordial noble gas carriers of different natures such as carbonaceous phases and iron sulfide minerals. This suggests that Q-gases may represent a ubiquitous noble gas reservoir outside the Sun at the time of the formation and accretion of the first solids in the protosolar nebula.

Acknowledgments

We are grateful to Maïa Kuga, Laurette Piani, Pete Burnard, Pierre-Henri Blard, Bernard Marty, Alice Williams, Barbara Marie, Laurent Rémusat and Matthias M.M. Meier for helpful discussions. The data for this paper are available by contacting Yves Marrocchi (yvesm@crpg.cnrs-nancy.fr). This is CRPG contribution #2333.

References

- Amari, S., et al. (2013), Highly Concentrated Nebular Noble Gases in Porous Nanocarbon Separates from the Saratov (L4) Meteorite, *Astrophys. J.*, 778, 37-45.
- Bourot-Denise, M., et al. (2010), Paris: The slightly altered, slightly metamorphosed CM that bridges the gap between CMs and COs., *Lunar and Planetary Science Conference XXXXI*, Lunar Planet. Inst., Houston, #1683 (abstr.).
- Brearley, A. J. (2006), The action of water, in *Meteorites and early solar system II*, edited by D. S. Lauretta and H. Y. McSween, pp. 587-624, Arizona University Press.
- Busemann, H., et al. (2000), Primordial noble gases in “phase Q” in carbonaceous and ordinary chondrites studied by closed system etching., *Meteorit. Planet. Sci.*, 35, 949-973.
- Clark, R. S., et al. (1967), Iodine, uranium and tellurium contents in meteorites, *Geochim. Cosmochim. Acta*, 31, 1605-1613.
- Crowther, S. A., and J. D. Gilmour (2013), The Genesis solar xenon composition and its relationship to planetary xenon signatures, *Geochim. Cosmochim. Acta*, 123, 17-34.

Crozaz, G. (1979), Uranium and thorium microdistributions in stony meteorites, *Geochim. Cosmochim. Acta*, 43, 127-133.

Derenne, S., and F. Robert (2010), Model of molecular structure of the insoluble organic matter isolated from Murchison meteorite, *Meteorit. Planet. Sci.*, 45, 1461-1475.

Gilmour, J. D., et al. (2006), The I-Xe chronometer and the early solar system, *Meteorit. Planet. Sci.*, 41, 19-31.

Gilmour, J. D. (2010), "Planetary" noble gas components and the nucleosynthesis history of solar system material., *Geochim. Cosmochim. Acta*, 74, 380-393.

Goles, G. G., and E. Anders (1962), Abundances of iodine, uranium and tellurium in meteorites, *Geochim. Cosmochim. Acta*, 26, 723-737.

Gros, J., and E. Anders (1977), Gas-rich minerals in the Allende meteorite: Attempted chemical characterization, *Earth Planet. Science Letters*, 33, 401-406.

Hewins, R. H., et al. (2014), The Paris meteorite, the least altered CM chondrite so far *Geochim. Cosmochim. Acta*, 124, 190-222.

Hohenberg, C. M., et al. (2002), Active capture and anomalous adsorption: New mechanisms for the incorporation of heavy noble gases. , *Meteorit. Planet. Sci.*, 37, 257-267.

Huss, G. R., et al. (1996), The "normal planetary" noble gas component in primitive chondrites: Compositions, carrier, and metamorphic history, *Geochim. Cosmochim. Acta*, 60, 3311-3340.

Huss, G. R., et al. (2006), Thermal metamorphism in chondrites, in *Meteorites and early solar system II*, edited by D. S. Lauretta and H. Y. McSween, pp. 567-586, Arizona University Press.

Kellerud, G. (1963), The Fe-Ni-S system, *Carnegie Inst. Washington Yearb.*, 62, 175-189.

Kerridge, J. F., et al. (1979), Iron-Nickel sulfides in the Murchison meteorite and their relationship to phase Q1, *Earth Planet. Science Letters*, 43, 1-4.

Lewis, R. S., et al. (1975), Host phase of a strange xenon component in Allende, *Science*, *190*, 1251-1262.

Lewis, R. S., et al. (1977), Xenon in Allende Sulfides and Other Recent Studies, *Meteoritics*, *12*(292-297).

Mabry, J., et al. (2007), Refinement and implications of noble gas measurements from Genesis., *Lunar and Planetary Science Conference XXXVIII*, Lunar. Planet. Inst., Houston, #1338 (asbtr.).

Marrocchi, Y., et al. (2005a), Interlayer trapping of noble gases in insoluble organic matter of primitive meteorites, *Earth and Planetary Science Letters*, *236*, 569-578.

Marrocchi, Y., et al. (2005b), Low-pressure adsorption of Ar, Kr, and Xe on carbonaceous materials (kerogen and carbon blacks), ferrihydrite, and montmorillonite: Implications for the trapping of noble gases onto meteoritic matter., *Geochim. Cosmochim. Acta*, *69*, 2419-2430.

Marrocchi, Y., et al. (2011), Adsorption of xenon ions onto defects in organic surfaces: Implications for the origin and the nature of organics in primitive meteorites., *Geochim. Cosmochim. Acta*, *75*, 6255-6266.

Marrocchi, Y., and G. Libourel (2013), Sulfur and sulfides in chondrules, *Geochim. Cosmochim. Acta*, *119*, 117-136.

Marrocchi, Y., and B. Marty (2013), Experimental determination of the xenon isotopic fractionation during adsorption, *Geophysical Research Letters*, *40*, 4165-4170.

Marrocchi, Y., et al. (2014), The Paris CM chondrite: Secondary minerals and asteroidal processing, *Meteorit Planet. Sci.*, *49*, 1232-1249.

Mathew, K. J., and K. Marti (2009), Galactic cosmic ray-produced ^{129}Xe and ^{131}Xe excesses in troilites of the Cape York iron meteorite, *Meteorit Planet. Sci.*, *44*, 107-114.

Matsuda, J.-I., et al. (2005), Primordial noble gases in a graphite-metal inclusion from the Canyon Diablo IAB iron meteorite and their implications, *Meteorit Planet. Sci.*, *40*(431-443).

Meshik, A. P., et al. (2007), Constraints on Neon and Argon Isotopic Fractionation in Solar Wind, *Science*, 318, 433-435.

Meshik, A. P., et al. (2014), Heavy noble gases in solar wind delivered by Genesis mission, *Geochim. Cosmochim. Acta*, 127, 326-347.

Nishimura, C., et al. (2008), Noble gas content and isotope abundances in phases of the Saint-Aubin (UNGR) iron meteorite, *Meteorit. Planet. Sci.*, 43, 1333-1350.

Ott, U., et al. (1981), Noble-gas-rich separates from the Allende meteorite, *Geochim. Cosmochim. Acta*, 45, 1751-1788.

Ozima, M., and F. A. Podosek (2002), *Noble gas geochemistry*, 286 pp., Cambridge University Press, Cambridge.

Piani, L., et al. (2012), Structure, composition, and location of organic matter in the enstatite chondrite Sahara 97096 (EH3), *Meteoritics & Planetary Science*, 47(1), 8-29.

Ragettli, R. A., et al. (1994), Uranium-xenon chronology: precise determination of $\lambda_{sf}^{*136}\text{Ysf}$ for spontaneous fission of ^{238}U , *Earth Planet. Science Letters*, 128, 653-670.

Tachibana, S., and G. R. Huss (2005), Sulfur isotope composition of putative primary troilite in chondrules from Bishunpur and Semarkona, *Geochim. Cosmochim. Acta*, 69, 3075-3097.

Verchovsky, A. B., et al. (2012), Separation of Q from Carbon in CR Meteorites During Stepped Combustion, in *Lunar and Planetary Science Conference*, edited, Houston.

Vogel, N., et al. (2004), Noble gases in chondrules and associated metal-sulfide-rich samples: Clues on chondrule formation and the behavior of noble gas carrier phases, *Meteorit. Planet. Sci.*, 39, 117-135.

Wieler, R., et al. (1992), Characterisation of Q-gases and other noble gas components in the Murchison meteorite, *Geochim. Cosmochim. Acta*, 56, 2907-2921.

Samples	Mass	Temperature	^{84}Kr (10^{-10} cc.g $^{-1}$)	$^{86}\text{Kr}/^{84}\text{Kr}$	^{132}Xe (10^{-10} cc.g $^{-1}$)	$^{129}\text{Xe}/^{132}\text{Xe}$
	(g)	(°C)				
FeS	0.0149	295	bdl	-	bdl	-
		591	bdl	-	bdl	-
		887	1.37	30.6 ± 0.4	0.76	194.6 ± 0.5
		1183	4.32	29.8 ± 0.3	1.82	245.5 ± 0.4
		1478	3.52	28.9 ± 0.3	0.68	173.3 ± 0.5
		1770	1.18	30.5 ± 0.4	0.21	103.6 ± 0.8
		Total	9.21	29.6 ± 0.3	3.27	218.5 ± 0.4
FeS-HCl	0.0173	291	bdl	-	bdl	-
		583	bdl	-	bdl	-
		875	1.18	30.2 ± 0.4	0.78	164.6 ± 0.6
		1166	2.07	29.9 ± 0.4	1.06	241.4 ± 0.4
		1458	1.08	29.8 ± 0.4	0.17	134.4 ± 0.8
		1770	0.82	30.5 ± 0.5	0.009	113.1 ± 1.1
		Total	4.33	30.0 ± 0.4	2.01	202.4 ± 0.5
FeS-	0.0126	291	bdl	-	bdl	-

HNO₃

583	bdl	-	bdl	-
875	0.61	30.9 ± 0.6	0.21	129.4 ± 1.8
1166	0.48	30.4 ± 0.6	0.21	141.2 ± 1.1
1458	0.43	30.0 ± 0.6	0.20	116.6 ± 1.2
1770	0.16	30.5 ± 0.7	0.16	106.4 ± 1.3
Total	1.52	30.5 ± 0.6	0.62	129.2 ± 1.3

Table 1: ⁸⁴Kr and ¹³²Xe concentrations and ⁸⁶Kr/⁸⁴Kr and ¹²⁹Xe/¹³²Xe isotopic ratios determined by stepwise heating of original pyrrhotite (FeS), HF/HCl-treated pyrrhotite (FeS-HCl) and nitric-etched pyrrhotite (FeS-HNO₃). Isotopic ratios ×100. bdl = below detection limit.

	Cold								
	Allende	Chainpur	Bokkeveld	Dimmit	Grosnaja	Isna	Lance	Murchison	Q
	CV3	LL3.4	CM2	H3.7	CV3	CO3.7	CO3.4	CM2	
I (ppm)	0.445	0.057	0.294	0.031	0.152	0.402	0.035	0.395	0.21
U (ppm)	50.07	2.06	0.02	0.56	5.53	33.98	2.55	43.29	9.63
¹²⁹ Xe from I decay (cc/g)	8.64 (-9)	1.03 (-9)	5.71 (-9)	6.13 (-10)	2.97 (-9)	7.80 (-9)	6.90 (-10)	7.67 (-9)	4.08 (-9)
¹³¹ Xe from U fission (cc/g)	6.25 (-12)	2.57 (-13)	2.49 (-15)	7.04 (-14)	6.90 (-13)	4.24 (-12)	3.19 (-13)	5.40 (-12)	1.20 (-12)
¹³² Xe from U fission (cc/g)	4.89 (-11)	2.01 (-12)	1.95 (-14)	5.51 (-13)	5.40 (-12)	3.32 (-11)	2.49 (-12)	4.23 (-11)	9.41 (-12)
¹³⁴ Xe from U fission (cc/g)	6.84 (-11)	2.81 (-12)	2.73 (-14)	7.71 (-13)	7.55 (-12)	4.64 (-11)	3.49 (-12)	5.91 (-11)	1.32 (-11)
¹³⁶ Xe from U fission (cc/g)	8.22 (-11)	3.38 (-12)	3.28 (-14)	9.26 (-13)	9.08 (-12)	5.58 (-11)	4.19 (-12)	7.11 (-11)	1.58 (-11)
¹²⁹ Xe from Pu fission	1.08 (-10)	4.43 (-12)	4.30 (-14)	1.21 (-12)	1.19 (-11)	7.30 (-11)	5.49 (-12)	9.30 (-11)	2.07 (-11)

	(cc/g)									
¹³¹ Xe from Pu fission										
	(cc/g)	5.56 (-10)	2.29 (-11)	2.22 (-13)	6.27 (-12)	6.14 (-11)	3.77 (-10)	2.84 (-11)	4.81 (-10)	1.07 (-10)
¹³² Xe from Pu fission										
	(cc/g)	2.00 (-9)	8.24 (-11)	8.00 (-13)	2.26 (-11)	2.21 (-10)	1.36 (-9)	1.02 (-10)	1.73 (-9)	3.85 (-10)
¹³⁴ Xe from Pu fission										
	(cc/g)	2.08 (-9)	8.58 (-11)	8.33 (-13)	2.35 (-11)	2.30 (-10)	1.42 (-9)	1.06 (-10)	1.80 (-9)	4.01 (-10)
¹³⁶ Xe from Pu fission										
	(cc/g)	2.24 (-9)	9.23 (-11)	8.95 (-13)	2.53 (-11)	2.48 (-10)	1.52 (-9)	1.14 (-10)	1.94 (-9)	4.31 (-10)

Table 2: Amounts of initial ^{238}U and ^{129}I required for correcting observed excesses of ^{129}Xe and $^{131,132,134,136}\text{Xe}$ in the Xe-Q of different chondrites and in the average Q composition relative to mass-fractionated SW-Xe (Data from [Busemann *et al.*, 2000; Wieler *et al.*, 1992]). Amounts of ^{129}Xe produced by the decay of ^{129}I at the concentrations required for correcting ^{129}Xe excesses observed relative to fractionated SW calculated from non-radiogenic/non-fissiogenic xenon isotopes. $^{129,131,132,134,136}\text{Xe}$ concentrations produced by the fission of ^{238}U and ^{244}Pu concentrations required to correct the observed excesses of $^{131,132,134,136}\text{Xe}$ in phase Q relative to mass-fractionated SW calculated from non-radiogenic/non-fissiogenic xenon isotopes and iodine-corrected ^{129}Xe (i.e., $^{124,126,128,129}\text{Xe}/^{130}\text{Xe}$). The number in bracket corresponds to the power.

Figure captions

Fig. 1: (a) ^{84}Kr elemental abundances determined by stepwise heating in the range 300-1768°C for original pyrrhotite (FeS), pyrrhotite that has undergone HF/HCl treatment (FeS-HCl) and etched pyrrhotite (FeS-HNO₃). (b) ^{132}Xe elemental abundances determined by stepwise heating in the range 300-1768°C for original pyrrhotite (FeS), HF/HCl residue (FeS-HCl) and pyrrhotite oxidized by HNO₃ (FeS-HNO₃).

Fig. 2: (a) Xe-Q composition normalized to the SW-Xe. Clear excesses of ^{129}Xe and $^{134,136}\text{Xe}$ are observed relative to a $\approx 10.1 \text{ ‰.amu}^{-1}$ mass-fractionated SW-Xe calculated from non-radiogenic/non-fissiogenic xenon isotopes (red line). These excesses are generally attributed to ^{129}I decay and to a contribution from an unidentified carrier with the same Xe-HL isotopic composition as HL-bearing nanodiamonds. (b) Modeled composition of Xe-Q corrected for the radiogenic and fissiogenic contributions of 0.21 ppm of ^{129}I and 9.63 ppm of ^{238}U , respectively. This model is compared to a recent model based on the mixing of fractionated SW-Xe with Xe-HL and Xe-S [*Meshik et al.*, 2014].

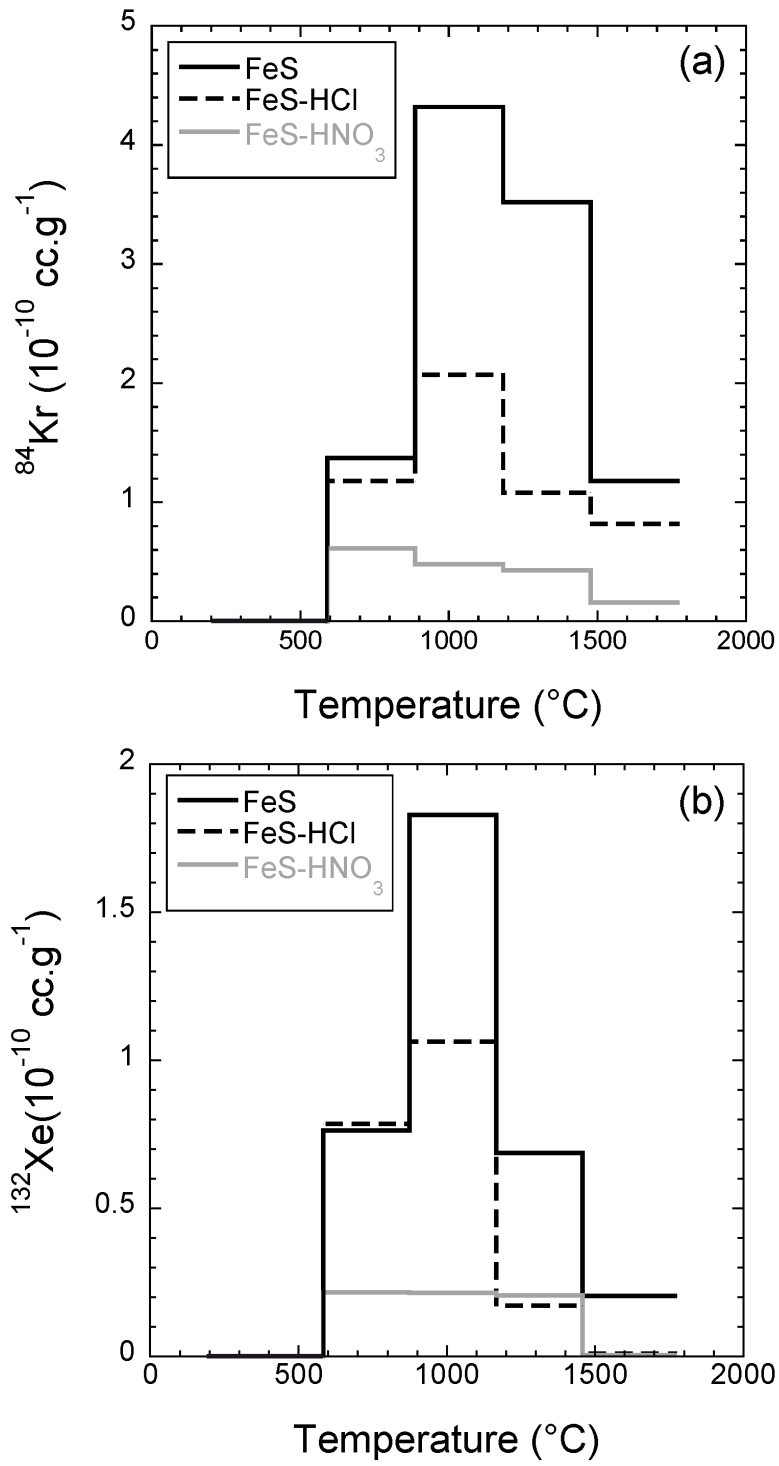


Fig. 1

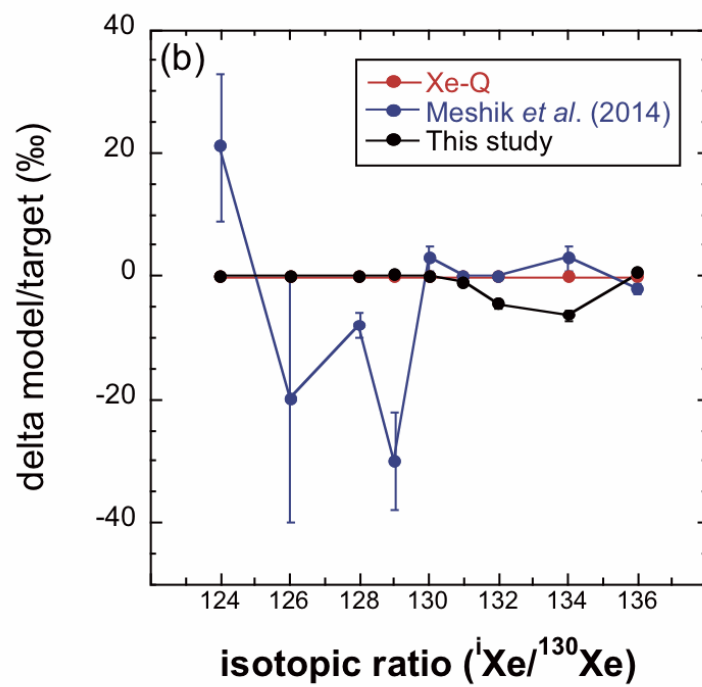
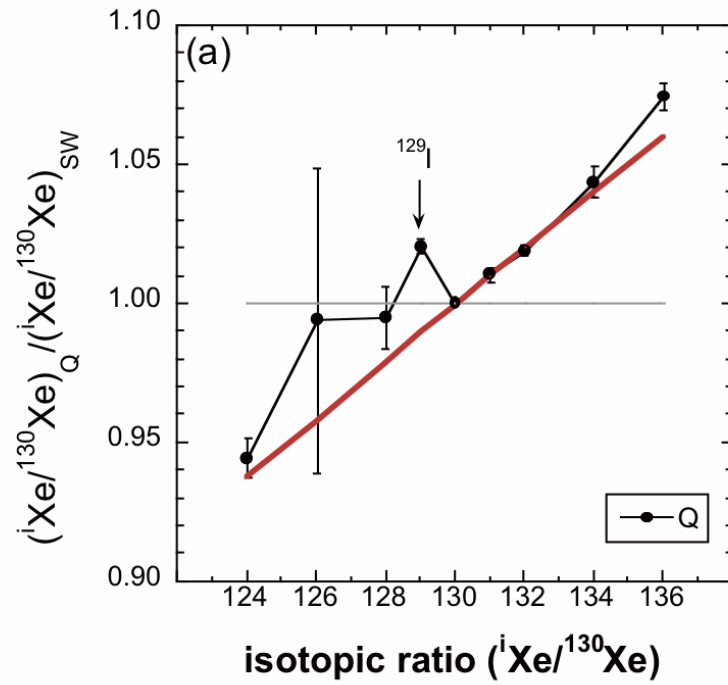


Fig. 2